Full length article

Blue light hazard optimization for white light-emitting diode sources with high luminous efficacy of radiation and high color rendering index

Jingjing Zhang [a,b], Weihong Guo [c], Bin Xie [b], Xingjian Yu [b], Xiaobing Luo [b,*], Tao Zhang [c], Zhihua Yu [a], Hong Wang [a], Xing Jin [a]

[a] *School of Automation, China University of Geosciences, Wuhan, Hubei 430074, China*
[b] *School of Energy and Power Engineering, Huazhong University of Science and Technology, Wuhan, Hubei 430074, China*
[c] *Shanghai Institute of Technical Physics, Chinese Academy of Sciences, Shanghai 200083, China*

ABSTRACT

Blue light hazard of white light-emitting diodes (LED) is a hidden risk for human's photobiological safety. Recent spectral optimization methods focus on maximizing luminous efficacy and improving color performances of LEDs, but few of them take blue hazard into account. Therefore, for healthy lighting, it's urgent to propose a spectral optimization method for white LED source to exhibit low blue light hazard, high luminous efficacy of radiation (LER) and high color performances. In this study, a genetic algorithm with penalty functions was proposed for realizing white spectra with low blue hazard, maximal LER and high color rendering index (CRI) values. By simulations, white spectra from LEDs with low blue hazard, high LER ($\geq$297 lm/W) and high CRI ($\geq$90) were achieved at different correlated color temperatures (CCTs) from 2013 K to 7845 K. Thus, the spectral optimization method can be used for guiding the fabrication of LED sources in line with photobiological safety. It is also found that the maximum permissible exposure duration of the optimized spectra increases by 14.9% than that of bichromatic phosphor-converted LEDs with equal CCT.

© 2017 Elsevier Ltd. All rights reserved.

1. Introduction

In recent years, phosphor-converted white light-emitting diodes (LEDs) have been widely used in street lighting and indoor illumination [1–3]. White LEDs offer great market potential for general illumination applications because of their merits of long lifetime, environmental friendliness, and high luminous efficiency. The white light from LEDs are mainly generated by a combination of blue light from blue chip and yellow light from phosphor. The spectral power distribution (SPD) implies high blue component ratio, which contains hidden blue hazard risk [4,5]. It has been proved that the hidden blue hazard risk of light sources brings damages to human's health [6–11]. Algvere et al. [6], Behar-Cohen [7] and Shen et al. [8] found that blue hazard risk brings huge damages to retinal. Tosini et al. [9] and Oh et al. [10] concluded that blue hazard risk could cause circadian disruption and hurts humans psychological health. Brainard et al. [11,12] argued that high blue hazard risk could lead to breast cancer for females.

Therefore, blue hazard of light source is a risk to photobiological safety.

In order to reduce blue hazard risk of light sources, blue component of SPD should be decreased. The color components of SPD have close relationship with correlated color temperature (CCT) and color rendering index (CRI), luminous efficacy (LE), which are key performances of light sources. Decreasing blue component may directly change the CCT and reduce the qualities of CRI and LE undesirably [13,14]. Many studies proposed different spectral optimization methods to solve the complicated relationships between color components, CCT, CRI, and LE for designing SPD of LEDs. However, previous spectral optimization methods focus on maximizing luminous efficacy and improving color performances of LEDs at different CCTs [15–17], few of them take blue hazard into account. Consequently, for photobiological safe illumination, there is an urgent need for proposing an easy and effective spectral optimization method to achieve spectra with low blue hazard, maximal luminous efficacy of radiation (LER), and high color performances at different CCTs. The spectral optimization method can be used for guiding the fabrication of LED sources in line with photobiological safety and promoting LEDs' wide application in indoor illumination.

---

* Corresponding author.
  E-mail address: luoxb@hust.edu.cn (X. Luo).

In this work, firstly, SPDs of eight most commonly used light sources in our daily life was tested, and the corresponding hidden blue hazard was analyzed. Then, a genetic algorithm (GA) with penalty functions was proposed to achieve white spectra with low blue hazard, maximal LER and high CRI values. Through numerous simulations, optimal spectra of the LED were obtained at different CCTs. Finally, the effectiveness of our method was verified by an illumination model.

2. Hidden blue hazard of light sources

Blue hazard spectral weighting function defined by the International Electrotechnical Commission (IEC) [18], shows blue hazard weighting to different wavelengths, is related with the hidden blue hazard. Photopic vision function proposed by the Commission Internationale de l'Eclairage (CIE) [19], which shows the human eye's visual response to different wavelengths, is relevant with luminous efficacy of light sources directly. The above two functions for wavelengths at 300–780 nm, are shown in Fig. 1. It is found that the maximal blue hazard function value is at 450 nm approximately, and maximal photopic vision function value is at 555 nm approximately. Since the intensities of the two functions are relatively very low for wavelengths at 300–380 nm than other wavelengths, we mainly discuss the visible wavelengths from 380 nm to 780 nm in the following parts.
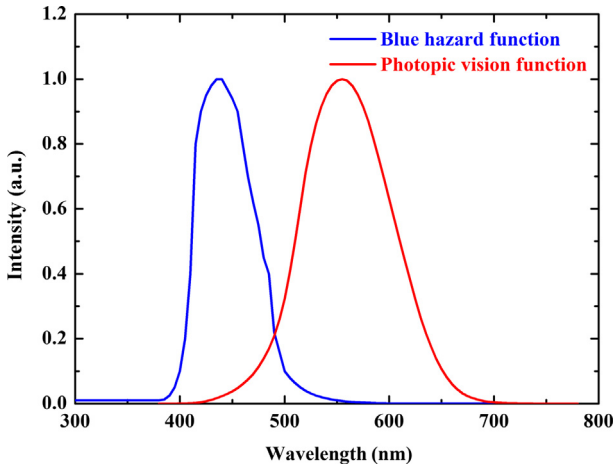
Therefore, the blue light hazard efficiency of radiation (BLHER), which is defined as the ratio of blue light hazard quantity to the corresponding radiometric quantity, can be expressed as [18]

$$\eta_B = \frac{\sum_\lambda S(\lambda)B(\lambda)\Delta\lambda}{\sum_\lambda S(\lambda)\Delta\lambda}, \tag{1}$$

where η_B is the blue light hazard efficiency of radiation, $S(\lambda)$ is the SPD of the light source, $B(\lambda)$ is the blue hazard spectral weighting function, $\Delta\lambda$ is the wavelength interval (5 nm in this work).

The LER can be expressed as [19]

$$LER = \frac{K_m\sum_\lambda S(\lambda)V(\lambda)\Delta\lambda}{\sum_\lambda S(\lambda)\Delta\lambda}, \tag{2}$$

where K_m, the maximal luminous flux of a light source, is 683 lm/W. $V(\lambda)$ is the photopic vision function.

Then, we analyzed SPDs of eight commonly used white light sources in our daily life, including three LED sources (backlight source of cellphone, backlight source of liquid crystal display (LCD) monitor, phosphor-converted (pc) LED), low pressure mercury lamp, and low pressure sodium lamp, FL1 fluorescent lamp, D65 solar illuminant, and incandescent light. The three LED sources were measured by a spectral illuminometer SPIC-200B (Everfine Inc., China), which offers spectral ranges from 380 to 780 nm and wavelength accuracy of 0.5 nm. The mercury lamp and the sodium lamp were measured by an integrating sphere spectrometer PMS-80 (Everfine Inc., China), which offers wavelength accuracy of 0.2 nm. All the results are tested at an ambient temperature of 25 °C. The SPDs of fluorescent lamp, D65 solar illuminant, and incandescent light were obtained from the CIE technical report [14]. The SPDs of LED sources for wavelengths from 380 nm to 780 nm at 5 nm intervals, are shown in Fig. 2(a). The SPDs of other illuminants for wavelengths from 380 nm to 780 nm, are shown in Fig. 2(b).

A blue hazard illumination model is used to analyze the hidden blue hazard of the SPDs, as shown in Fig. 3. A light source with the above SPD illuminates the illuminated surface at a vertical angle. d is the distance between the emitting center and the illuminated surface, φ is the half emitting angle, S is the area of the illuminated surface, Ω is the solid angle from the emitting center to the illuminated surface.

The spectral radiance of the light source can be calculated as [20]

$$L(\lambda) = \frac{S(\lambda)}{S\Omega} = \frac{S(\lambda)}{\pi(d\tan\varphi)^2 2\pi(1-\cos\varphi)}\,\text{W m}^{-2}\,\text{sr}^{-1}, \tag{3}$$

Fig. 1. Blue hazard spectral weighting function and photopic vision function referring to wavelengths from 300 nm to 780 nm.

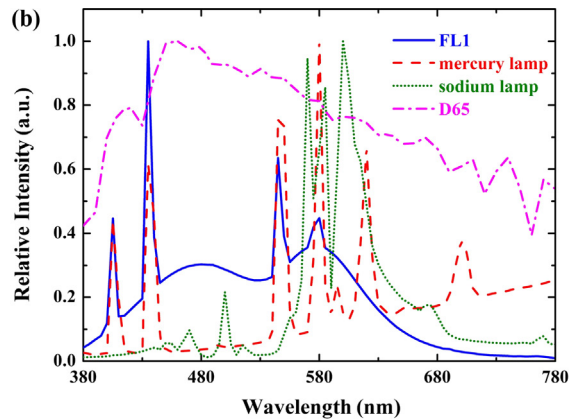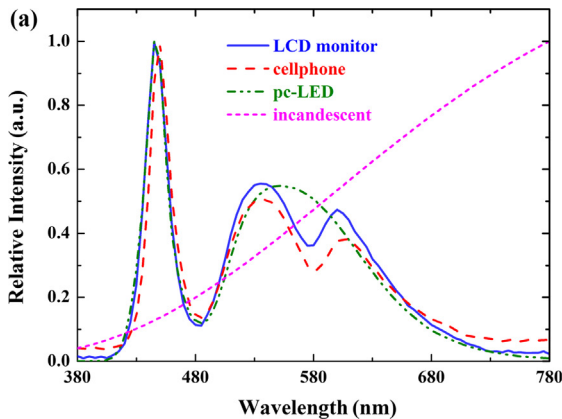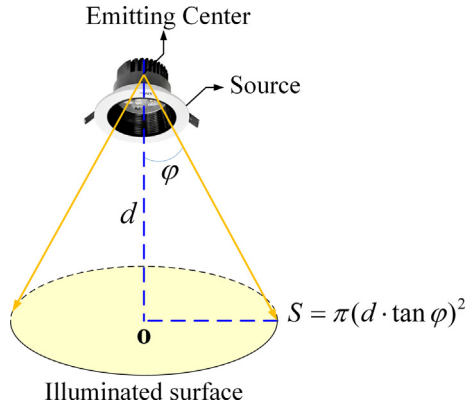**Fig. 2.** SPDs of eight white light sources for (a) LEDs and (b) other illuminants.

Fig. 3. The blue hazard illumination model.

where Ω can be calculated as $\Omega = 2\pi(1 - \cos\varphi)$. Here, it is supposed that the radiant power of the light source is 100 W, and d is 200 mm. And after an optical design, the radiance of the illuminated surface is uniform in the model.

The radiant flux that enters the eye and is absorbed by the retina is proportional to the pupil area. It is known that the pupil diameter decreases from around 7 mm diameter at very low luminance (<0.01 cd m^{-2}) to about 2 mm at luminance values on the order of 10,000 cd m^{-2} [21]. For the blue light hazard assessment, a 3 mm pupil diameter (7 mm^2 area) was used to derive the exposure limit [18]. To avoid retinal photochemical injury from chronic blue-light exposure, two exposure limit values are proposed based on the best available information from experimental studies [6,22]. One is the integrated spectral radiance of the light source weighted against the blue-light hazard function, i.e., the blue light weighted radiance, L_B, shall not exceed the levels defined by [18]

$$\begin{cases} L_B t = \sum_\lambda L(\lambda)B(\lambda)\Delta\lambda t \leqslant 10^6 \text{ J m}^{-2} \text{ sr}^{-1} \text{ (for } t \leqslant 10^4 \text{ s)} \\ L_B = \sum_\lambda L(\lambda)B(\lambda)\Delta(\lambda) \leqslant 100 \text{ W m}^{-2} \text{ sr}^{-1} \text{ (for } t > 10^4 \text{ s)} \end{cases}, \quad (4)$$

where t is the exposure duration in seconds. The other is, for a weighted source radiance exceeding 100 W m^{-2} sr^{-1}, the maximum permissible exposure duration, t_{max}, can be computed as [18]

$$t_{\max} = \frac{10^6}{L_B} \text{ s (for } t \leqslant 10^4 \text{ s)} \quad (5)$$

The above two exposure limits apply to nearly all individuals in the general population may be repeatedly exposed without adverse health effects [18]. However, they do not apply to abnormally photosensitive individuals or to individuals concomitantly exposed to photosensitizing agents, which makes individuals much more susceptible to adverse health effects from optical radiation. The susceptibility of photosensitive individuals varies greatly, and it is not possible to set exposure limits for this portion of the population [23,24].

The CCT, general CRI (R_a), BLHER (η_B), LER, L_B at $\varphi = 5°$, and the corresponding t_{max} of the eight SPDs are calculated as shown in Table 1.

It is concluded that the CCTs of the common used light sources varies from 1837 K to 6746 K, the R_a varies from 31 to 100, LER varies from 203 to 334 lm/W, η_B varies from 0.04 to 0.27. The PC-LED has the highest LER (322 lm/W), but its maximum permissible exposure time is as short as 956 s, which indicates it has a high hidden blue hazard. On the other side, the incandescent light has the lowest η_B (0.05) and longest maximum permissible exposure time, but its LER is much lower (154 lm/W) than that of other sources, which indicates the light source is not energy-saving. Consequently, light sources with optimized spectra for highest LER, lowest η_B and high R_a at different desired CCTs are in urgent need. Since LED is widely accepted as most suitable for spectrum tuning and optimization [15–17], we optimized LED spectra for realizing highest LER, lowest η_B, high R_a at different desired CCTs.

3. Spectral optimization method

To achieve high LER and R_a values, most light sources in the literature report fabricating phosphor-converted white LEDs integrated with red phosphor, red chromatic LEDs or semiconductor colloidal quantum dots (QDs) [25–27]. The QDs are more suitable for spectrum tuning due to their narrow emission spectra. Therefore, our spectral model of white LEDs consists of blue chips (narrowband radiation), yellow phosphors (broadband radiation), and red phosphor, red chips or quantum dots (narrowband radiation). The relative SPD of white LEDs, $S_W(\lambda)$, is given by

$$S_W(\lambda) = p_b S(\lambda, \lambda_b, \Delta\lambda_b) + p_y S(\lambda, \lambda_y, \Delta\lambda_y) + p_r S(\lambda, \lambda_r, \Delta\lambda_r) \quad (6)$$

where $S(\lambda, \lambda_b, \Delta\lambda_b)$, $S(\lambda, \lambda_y, \Delta\lambda_y)$, and $S(\lambda, \lambda_r, \Delta\lambda_r)$ refer to the relative SPDs of blue chips, yellow phosphors, and red chips or quantum dots, λ_b, λ_y, and λ_r refer to the peak wavelengths of the blue, yellow, and red color components, $\Delta\lambda_b$, $\Delta\lambda_y$, and $\Delta\lambda_r$ refer to the full widths at half maximum (FWHMs) of the three color components, and p_b, p_y, and p_r designate the proportions of the relative spectra of the three color components, respectively. The above spectral parameters, including peak wavelengths, FWHMs and proportions, comprise a 3×3-dimensional parameter matrix. The blue and red radiation can be described as a modified Gaussian distribution, which is given by Ohno [28]. The yellow radiation is approximated by a Gaussian distribution in this analysis [29]. The FWHM of blue chip varies from 20 nm to 50 nm [30], the FWHM of green phosphors varies from 80 nm to 120 nm [31,32], and the FWHM of red component varies from 20 nm to 100 nm [28,33]. Wavelengths for each color component vary from 380 nm to 500 nm for blue, 500 nm to 600 nm for yellow, and 600 nm to 780 nm for red. The relative spectra of the three color components are normalized and the proportions of the relative spectra vary from 0 to 1. Thus, the spectral shapes concerning each specific band are considered in the formula.

Table 1
The performances of eight SPDs.

Light source	CCT (K)	R_a	LER (lm/W)	η_B	L_B (W m^{-2} sr^{-1} nm^{-1})	t_{max} (s)
Sodium lamp	1837	31	334.11	0.04	172.80	5787
Incandescent	2857	100	154.14	0.05	189.19	5286
Mercury lamp	3204	64	222.00	0.11	441.55	2265
PC-LED	5902	71	322.34	0.26	1045.54	956
LCD monitor	6030	81	305.12	0.25	1012.03	988
Fluorescent	6430	74	292.25	0.27	1075.01	930
D65	6504	98	203.52	0.20	754.29	1326
Cellphone	6746	85	279.68	0.25	997.58	1002

To obtain a low blue hazard and energy-saving light source, η_B and LER should be taken into account simultaneously. Therefore, a spectral optimization method was proposed for boosting the maximum attainable LER and minimum η_B at high CRI values and at various CCTs by varying the parameter matrix in the SPD model. In addition, it is important that the chromaticity difference from the Planckian locus on the CIE 1960 uv chromaticity diagram (D_{uv}) be smaller than 0.0054 for various CCTs [25]. We maximize the LER and minimize the η_B under the constraints of CRI, CCT, and D_{uv} simultaneously.

$$\begin{cases} \text{Maximum}: LER; \text{ Minimum}: \eta_B \\ \text{Constraints}: R_a \geqslant R_{as}, D_{uv} \leqslant 0.0054, \frac{|CCT-CCT_{tar}|}{CCT_{tar}} \leqslant 0.02 \end{cases}, \quad (7)$$

where LER and η_B are the direct optimization goals, the objective function $f(\vec{x})$ can be expressed as linear weighted model of LER and η_B. R_{as} is the optimization constraints referring to the general CRI (R_a). Here, R_{as} is assigned as 90. CCT_{tar}, the designated value of CCT, varies from 2000 K to 8000 K at an interval of 1000 K. In our optimization, the constraint of deviation between the actual CCT and CCT_{tar} is less than 2%.

Therefore, this is a multi-object optimization problem with inequality constraints. The genetic algorithm (GA) has been proven for having faster global convergence and higher computational efficiency than other optimization methods [34,35]. Besides, the penalty function approach is generic and applicable to many types of constraint [36,37]. In this paper, therefore, we adopted a genetic algorithm (GA) for calculating the maximum value of LER and minimum value of η_B. And penalty functions, $g_j(\vec{x})$ ($j = 1, 2, 3$), are used to handle the inequality constraints in Eq. (6), referring to R_a, D_{uv} and CCT [17]. Here, the objective function $f(\vec{x})$ can be expressed as linear weighted model of LER and η_B. The theoretical maximum value of η_B is 1 and the theoretical maximum value of LER is 683 lm/W. In order to reduce both the mutual influence of η_B

Table 2
Results of simulations.

CCT (K)	R_a	D_{uv}	η_B	LER (lm/W)
2013	90	0.0054	0.02	352
2940	90	0.0054	0.08	350
3929	90	0.0054	0.15	344
5000	90	0.0054	0.21	330
5880	90	0.0054	0.23	302
6860	92	0.0054	0.25	297
7845	92	0.0054	0.28	280

and LER, they are normalized in $f(\vec{x})$. The fitness function $F(\vec{x})$ of the GA, defined as the sum of the objective function $f(\vec{x})$ and the penalty terms $R_jg_j(\vec{x})$ which depend on the constraints, can be expressed as

$$\begin{cases} F(\vec{x}) = f(\vec{x}) + \sum_j R_jg_j(\vec{x}), \; j = 1, 2, 3 \\ f(\vec{x}) = A\eta_B + (1-A)\left(\frac{683-LER}{683}\right) \\ g_1(\vec{x}) = \frac{R_a - R_{as}}{R_{as}} \\ g_2(\vec{x}) = \frac{D_{uv} - 0.0054}{0.0054} \\ g_3(\vec{x}) = \frac{|CCT-CCT_{tar}|/CCT_{tar} - 0.02}{0.02} \end{cases}, \quad (8)$$

where R_j is the penalty parameter which is a very large positive number, A is the linear weighting coefficient of the η_B and LER, varies from 0 to 1 at an interval of 0.05 during the optimization. In order to reduce both the mutual influence of LER, η_B, R_a, D_{uv} and CCT in the fitness function $F(\vec{x})$, R_a, D_{uv} and CCT in the penalty functions $g_j(\vec{x})$ are also normalized in Eq. (8).

As the penalty parameter R_j is a very large positive number, when R_a, D_{uv}, or CCT do not meet the constraints, the fitness function $F(\vec{x})$ will be a much larger positive number than in the case when all the constraints are met. Thus, the GA evolutionary process will force the solution of the equation to approach the feasible solution that meets the constraints by varying the chromosomes [17,37]. Here, the GA parameters are as follows: the number of chromosomes is 40, the precision of chromosomes is 25, the penalty parameter R_j is 2000, the generation gap is 0.9, and the probability of crossover occurring between pairs of chromosomes is 0.7. Determining whether the fitness function satisfies the stop conditions, which can be of two kinds. One is the number of evolution generations reaches 50,000; the other is the lowest fitness function in each chromosome group does not change over 500 generations.

4. Results and discussions

By conducting numerous simulations, the optimal spectral parameters of each color component and their performances with $R_a \geq 90$, at CCTs from 2013 K to 7845 K for maximal LER, have been obtained by maximizing $F(\vec{x})$. The simulation results are listed in Table 2.

It is found that the optimal spectra at different desired CCTs exhibits high color performance and energy-saving performance in which $R_a \geq 90$, $LER \geq 297$ lm/W, with the D_{uv} meeting the
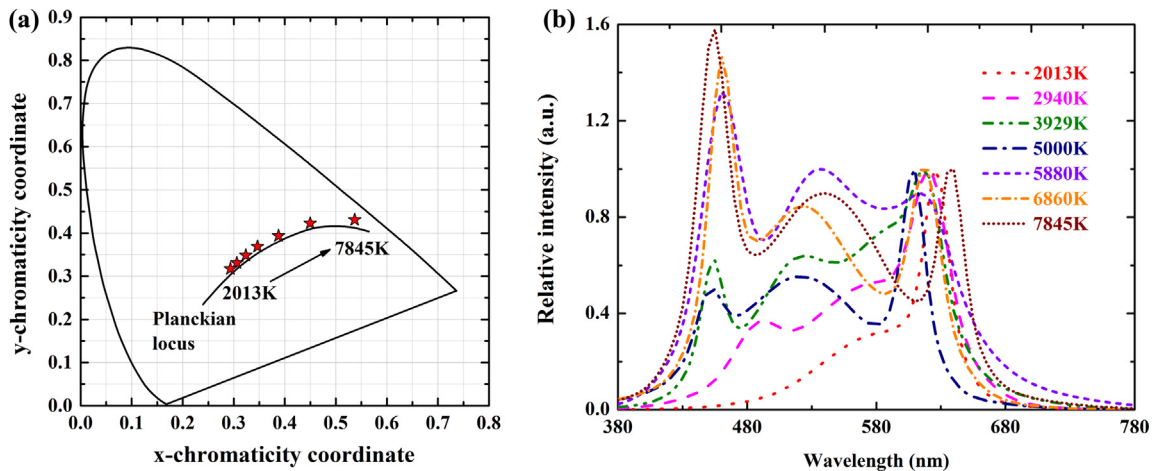

Fig. 4. Optimization results for (a) chromaticity coordinate diagram and (b) spectra.

constraints $D_{uv} \leq 0.0054$. The chromaticity of the optimized spectra are shown in Fig. 4(a), the corresponding spectra with different CCTs are shown in Fig. 4(b).

The general CRI (R_a) is simply the average of special CRIs (R_i) for the first eight samples. A perfect score of 100 represents no color differences in the samples under the test source and reference illuminant [13]. Fig. 5 shows the eight special CRIs comparison between the optimized LED at CCT = 5880 K and the commercial pc-LED tested in Section II (CCT = 5902 K). The CCTs of the two sources are approximately equal and the CRIs of the optimized LED is much higher than that of the pc-LED. It is concluded that the color rendering index of optimized LED is improved by our optimization.

The η_B and LER varying with increasing CCTs are shown in Fig. 6. It is found that LER decreases from 352 lm/W to 280 lm/W, and η_B increases from 0.02 to 0.28 when CCT increases from 2013 K to 7845 K, respectively. In order to analyze the blue hazard of the optimal spectra in detail, we use the blue hazard illumination model proposed in Section 2.

According to Eq. (5), we calculated the L_B of the optimized spectra at half emitting angles of 5°, 15°, 30°, 45°, and 60°. The calculated data are shown in Fig. 7. It is concluded that the L_B increases with increasing CCTs, and decreases with increasing half emitting angles. The L_B are greater than 100 W m^{-2} sr^{-1} at CCTs from 2940 K to 7845 K when φ is 5°, so we calculate the t_{max} by formula (5), referring to 2961 s, 1643 s, 1192 s, 1098 s, 979 s, 898 s, respectively. L_B decreases from 910.43 to 3.26 with increasing φ at CCT = 5880 K. Therefore, the hidden blue hazard of LED source increases with increasing CCTs, and decreases with increasing emitting angles.

The bichromatic PC-LED with CCT = 5902 K exhibits performance in which R_a = 71, t_{max} = 956 s, and the optimal spectrum at CCT = 5880 K exhibits performance in which R_a = 90, t_{max} = 1098 s. It is found that the CCTs of the above two light sources are approximately equal, the CRI increases from 71 to 90. More importantly, the maximum permissible exposure duration t_{max} of the optimal spectrum has been increased by 14.9% referring to that of PC-LED. Therefore, the photobiological safety performance of white light source can be improved by our method.

In addition, the simulation results are compared with our previous study without considering hidden blue hazard of LED source [17]. In our previous study, we proposed spectral optimization by boosting the maximum attainable LER of spectra while constraining high color performance. When CCT is 5940 K, R_a is 95, and the η_B is 0.24. We calculate the t_{max} when φ is 5°, referring to
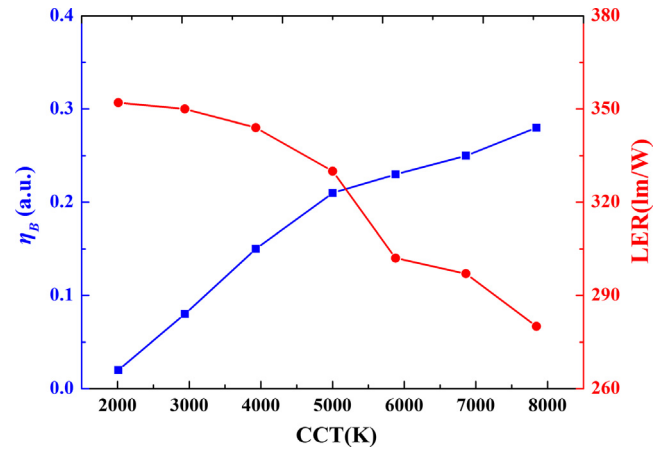

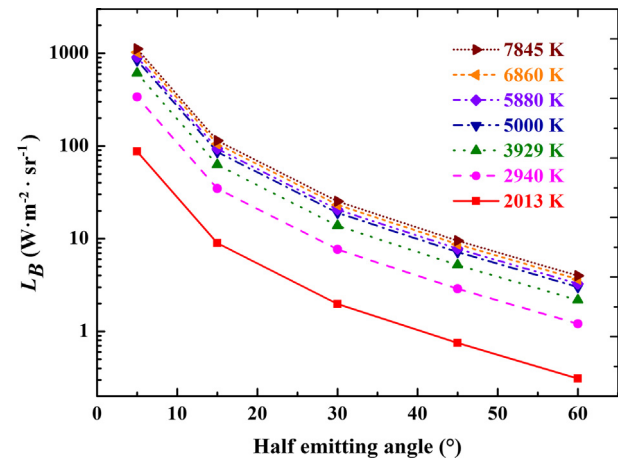**Fig. 6.** Optimization results for η_B and LER at CCTs from 2013 K to 7845 K.

Fig. 7. L_B of the optimized spectra at different half emitting angles.

1044.9 s. The maximum permissible exposure duration t_{max} of the current optimal spectrum increases by 5.1% referring to that of our previous method.

Further, the simulation was conducted at different desired LERs (270 lm/W, 300 lm/W, 330 lm/W) with the constraints of $R_a \geq 90$.
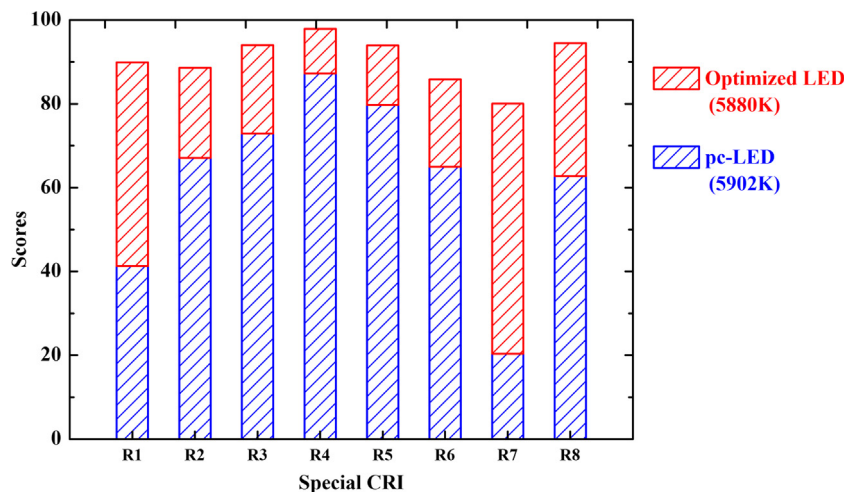

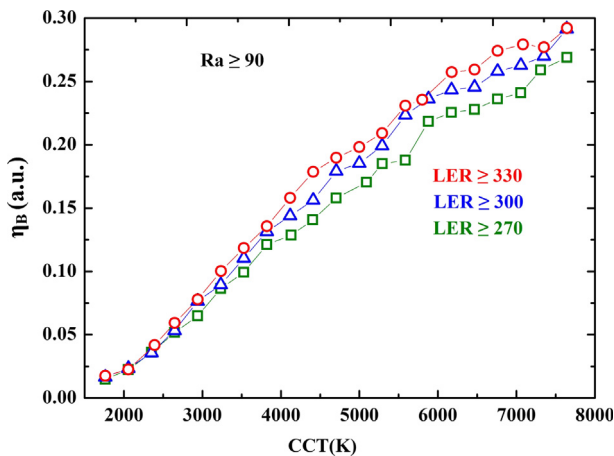**Fig. 5.** The eight special CRIs of the optimized LED at CCT = 5880 K and the commercial pc-LED.

Fig. 8. The minimum η_B of trichromatic white LED at different desired LERs.

The minimum η_B of trichromatic white LED with CCTs from 1800 K to 7800 K at a 300 K interval are shown in Fig. 8.

It is found that the minimum hidden blue hazard increases with increasing CCTs at an equal desired LER. The minimum η_B increases from 0.015 to 0.269 with CCTs increases from 1800 K to 7800 K at $LER \geq 270$ lm/W, from 0.016 to 0.269 at $LER \geq 300$ lm/W, and from 0.017 to 0.292 at $LER \geq 330$ lm/W. Moreover, the minimum η_B increases with LER increases from 270 lm/W to 330 lm/W.

5. Conclusions

SPDs of eight most commonly used light sources in our daily life was tested, and the corresponding hidden blue hazard was analyzed. The common used light sources are proved not have both high LER, high CRI and low blue hazard. Then, a genetic algorithm (GA) with penalty functions was proposed to achieve trichromatic LED spectra with low blue hazard, maximal LER and high CRI values. Through numerous simulations, optimal spectra of the LED with high LER ($\geq$297 lm/W) and high CRI ($\geq$90) were obtained at CCTs from 2013 K to 7845 K. It is found that the maximum permissible exposure duration t_{max} of the optimal spectrum is increased by 14.9%, referring to that of bichromatic phosphor-converted LEDs with equal CCT. Moreover, the minimum hidden blue hazard of LED increases with increasing CCTs and increasing LERs. The spectral optimization method presents a great potential for guiding the fabrication of LED sources in line with photobiological safety, and paves the way for LEDs' wide application in indoor illumination.

Acknowledgments

References

[1] E.F. Schubert, J.K. Kim, Solid-state light sources getting smart, Science 308 (5726) (2005) 1274–1278.
[2] Y.P. Ma, R. Hu, X.J. Yu, W.C. Shu, X.B. Luo, A modified bidirectional thermal resistance model for junction and phosphor temperature estimation in phosphor-converted light-emitting diodes, Int. J. Heat Mass. 106 (2017) 1–6.
[3] X.B. Luo, R. Hu, S. Liu, K. Wang, Heat and fluid flow in high-power LED packaging and applications, Prog. Energy Combust. Sci. 56 (2016) 1–32.
[4] T. Lougheed, Hidden blue hazard? LED lighting and retinal damage in rats, Environ. Health Persp. 122 (3) (2014), A81-A81.
[5] W.T. Ham, H.A. Mueller, D.H. Sliney, Retinal sensitivity to damage from short wavelength light, Nature 260 (5547) (1976) 153–155.
[6] P.V. Algvere, J. Marshall, S. Seregard, Age-related maculopathy and the impact of blue light hazard, Acta Ophthalmol. 84 (1) (2006) 4–15.
[7] F. Behar-Cohen, C. Martinsons, F. Vienot, G. Zissis, A. Barlier-Salsi, J.P. Cesarini, O. Enouf, M. Garcia, S. Picaud, D. Attia, Light-emitting diodes (LED) for domestic lighting: any risks for the eye?, Prog Retin. Eye Res. 30 (4) (2011) 239–257.
[8] Y. Shen, C. Xie, Y. Gu, X. Li, J. Tong, Illumination from light-emitting diodes (LEDs) disrupts pathological cytokines expression and activates relevant signal pathways in primary human retinal pigment epithelial cells, Exp. Eye Res. 145 (2016) 456–467.
[9] G. Tosini, I. Ferguson, K. Tsubota, Effects of blue light on the circadian system and eye physiology, Mol. Vis. 22 (2016) 61–72.
[10] J.H. Oh, H. Yoo, K. Park, Y.R. Do, Analysis of circadian properties and healthy levels of blue light from smartphones at night, Sci. Rep. 5 (2015) 11325.
[11] G. Glickman, R. Levin, G.C. Brainard, Ocular input for human melatonin regulation: relevance to breast cancer, Neuro Endocrinol. Lett. 23 (1) (2002) 17–22.
[12] R.G. Stevens, G.C. Brainard, D.E. Blask, S.W. Lockley, M.E. Motta, Breast cancer and circadian disruption from electric lighting in the modern world, CA Cancer J. Clin. NLM 64 (3) (2014) 207–218.
[13] Commission Internationale de l'Eclairage, "Color rendering of white LED light sources," Technical Report CIE 177, 2007.
[14] Commission Internationale de l'Eclairage, "Colormetry," Technical Report CIE 15, 2005.
[15] Q. Dai, L. Hao, Y. Lin, Z. Cui, Spectral optimization simulation of white light based on the photopic eye-sensitivity curve, J. Appl. Phys. 119 (5) (2016) 053103.
[16] L.L. Zan, D.Y. Lin, P. Zhong, G.X. He, Optimal spectra of white LED integrated with quantum dots for mesopic vision, Opt. Express 24 (7) (2016) 7643–7653.
[17] J.J. Zhang, R. Hu, X.J. Yu, B. Xie, X.B. Luo, Spectral optimization based simultaneously on color-rendering index and color quality scale for white LED illumination, Opt. Laser Technol. 88 (2017) 161–165.
[18] Internation Electrotechnical Comission, "Photobiological safety of lamps and lamp systems," International Standard IEC 62471, 2006.
[19] Commission Internationale de l'Eclairage, "2° Spectral Luminous Efficiency Function for Photopic Vision," Technical Report CIE 086, 1990.
[20] H. Hashemi, K. Yazdani, M. Khabazkhoob, S. Mehravaran, K. Mohammad, A. Fotouhi, Distribution of photopic pupil diameter in the Tehran eye study, Curr. Eye Res. 34 (5) (2009) 378–385.
[21] Internation Electrotechnical Comission, "Application of IEC 62471 for the assessment of blue light hazard to light sources and luminaires," Technical Report IEC 62778, 2012.
[22] D.H. Sliney, Eye protective techniques for bright light, Opthalmology 90 (8) (1983) 937–944.
[23] International Commission on Non-Ionizing Radiation Protection, Guidelines on limits of exposure to broadband incoherent optical radiation (0.38–3 μm), Health Phys. 73 (1997) 539–554.
[24] American National Standard Institute/Illuminating Engineering Society of North America, "Recommended practice for photobiological safety for lamps - general requirements", New York, IESNA, 1996.
[25] J.H. Oh, Y.J. Eo, S.J. Yang, Y.R. Do, High-color-quality multipackage phosphor-converted LEDs for yellow photolithography room lamp, IEEE Photonics J. 7 (2) (2015) 1300308.
[26] T. Erdem, Y. Kelestemur, Z. Soran-Erdem, Y. Jin, H.V. Demir, Energy-saving quality road lighting with colloidal quantum dot nanophosphors, Nanophotonics 3 (6) (2014) 373–381.
[27] H.T. Li, X.L. Mao, Y.J. Han, Y. Luo, Wavelength dependence of colorimetric properties of lighting sources based on multi-color LEDs, Opt. Express 21 (3) (2013) 3775–3783.
[28] Y. Ohno, Spectral design considerations for color rendering of white LED sources, Opt. Eng. 44 (11) (2005) 111302.
[29] C. Sommer, F.P. Wenzl, P. Hartmann, P. Pachler, M. Schweighart, S. Tasch, G. Leising, Tailoring of the color conversion elements in phosphor-converted high-power LEDs by optical simulations, IEEE Photonics Technol. Lett. 20 (9) (2008) 1041–1135.
[30] H. Jin, S. Jin, K. Yuan, S. Cen, Two-Part Gauss simulation of phosphor-coated LED, IEEE Photonics J. 5 (4) (2013) 1600110.
[31] W. Davis, Y. Ohno, Color quality scale, Opt. Eng. 49 (3) (2010) 033602.
[32] Y. Lin, Z. Deng, Z. Guo, Z. Liu, H. Lan, Y. Lu, Y. Cao, Study on the correlations between color rendering index and the spectral power distribution, Opt. Express 22 (S4) (2014) A1029–A1039.
[33] B. Xie, R. Hu, X.B. Luo, Quantum dots-converted light-emitting diodes packaging for lighting and display: status and perspectives, J. Electron. Packaging 138 (2) (2016) 020803.
[34] F.G. Tari, Z. Hashemi, A priority based genetic algorithm for nonlinear transportation costs problems, Comput. Ind. Eng. 96 (2016) 86–95.
[35] O. Dib, M. Manier, L. Moalic, A. Caminada, Combining VNS with genetic algorithm to solve the one–to-one routing issue in road networks, Comput. Oper. Res. 78 (2017) 420–430.
[36] J.J. Zhang, R. Hu, B. Xie, X.J. Yu, X.B. Luo, Z.H. Yu, L.J. Zhang, H. Wang, X. Jin, Energy-saving light source spectrum optimization by considering object's reflectance, IEEE Photonics J. 99 (1) (2017) 2658606.
[37] K. Deb, An efficient constraint handling method for genetic algorithms, Comput. Method Appl. Mech. Eng. 186 (2) (2000) 311–338.